Fluid Flow Patterns and Velocity Distribution on Commercial-Scale Sieve Trays

A fluorimetric technique was used to determine detailed residence time and velocity distribution on commercial sieve trays installed in a five-tray, 1.22 m dia. air/water simulator. Results show a strong effect of the gas rate on the residence time distribution. At low air rates, isochron lines of high residence time are found at the column wall, and the variance distributions suggest the existence of zones of different degrees of mixing. The velocity profiles at F_s (vapor velocity load) factors less than 0.65 show severe flow nonuniformities characterized by a high velocity at the centerline and stagnant zone close to the wall. At higher F_s factors the velocity maldistribution seems to be relatively mild. Correlations are presented to estimate the velocity distribution on the tray as a function of the gas rate.

R. B. SOLARI and R. L. BELL

Department of Chemical Engineering
University of California
Davis, CA 95616

SCOPE

The use of sieve and valve trays is very common in current-design distillation units. Most of the information on large size tray design is given in the form of empirical correlations obtained from pilot plants, which do not take in account the actual flow patterns on the tray. This type of correlation is so widespread that Bolles (1976) has recommended using the same correlations to estimate the efficiency of both sieve and valve trays. Garret et al. (1977) have also assumed similar mixing characteristics for the two types of trays. However, it has been shown that flow and mixing patterns are highly dependent on tray design and flow conditions (Bell, 1972a; Aleksandrov and Vybornov, 1971; Porter et al., 1972); therefore it should be expected to find different tray performance for different designs. The type of liquid flow configurations found in large size trays include liquid channeling, by-passing, nonuniform velocity distribution, stagnant zones, and flow recirculation. Fell and Pinczewski (1977) have also noted that an industrial sieve tray of a given design may operate in one of a number of hydrodynamic regimes depending on vapor and liquid loading, which in turn will influence tray efficiency. However, none of these types of flow nonuniformities have been considered in the current methods of tray prediction. Throughout the literature the underlying assumption regarding fluid motion has been that of a uniform rectilinear velocity field with superimposed eddy mixing effect. Nonuniform flow patterns have not been included in the tray efficiency prediction mainly because there have been only a few serious attempts to measure the actual flow patterns (Bell, 1972a; Alexandrov and Vybornov, 1976; Weiler et al., 1973; Solari et al., 1982; Sohlo and Kinnunen, 1977). So far, it is not clear from the data reported in the literature what type of flow configuration can be expected for a given type of design for a set of operating conditions, and the liquid velocity distributions on the tray still remain unknown.

Bell and Solari (1974) have shown that a simple nonuniform velocity distribution, even in those cases where mixing is not an important factor, can substantially reduce the tray efficiency. If retrograde flow is present, depending on the intensity of velocity maldistribution, the efficiency is further affected. In severe cases, it was shown that ratios of Murphree tray efficiency to point efficiency (EMV/EOC) less than unity were possible. In the model used for these calculations the parameters involved were related to the velocity distribution including retrograde flow and stagnant zones.

The objectives of the study presented here were to determine the effect of liquid and vapor flow on mixing and flow patterns on an industrial sieve tray, to measure velocity distribution, and to evaluate the parameters of the retrograde flow model presented in our previous papers (Bell and Solari, (1974), Solari and Bell (1978)). A five-tray, commercial-scale air/water simulator was used to determine detailed residence time and velocity distribution on commercial sieve trays. A fluorimetric technique, in which the response of the system to a pulse injection of fluorescent dye could be measured at a point, was used. The experimental data obtained were used to evaluate the adjustable parameters of the retrograde flow model and to compare tray efficiency predictions for industrial services reported in the literature.

CONCLUSIONS AND SIGNIFICANCE

The residence time distributions are strongly affected by the gas rate and show extended residence time near the wall and relatively shorter residence time near the centerline.

These results are qualitatively identical to those reported by Bell (1972b) for trays in hydrocarbon service, and they indicate severe flow nonuniformities in the tray. The variance distributions show characteristics very similar to the residence time distribution and they suggest the existence of zones of

* The present address of R. B. Solari is INTEVEP, S. A., Caracas, Venezuela.

different degrees of lateral mixing on the tray, specifically at low gas rates. No significant retrograde flow was found with the tray design being studied except for F_s factors below about 0.65. Even under these conditions, the zones were more like stagnant areas with some degree of back-mixing than like true retrograde flow zones. The fact that strong evidence of flow recirculation was found in the absence of air flow indicates that the gas rate has a strong influence in shaping the liquid flow patterns on the tray.

Linear velocity distributions were measured with ±10% accuracy. The velocity profiles at F_s factors less than 0.65 show severe flow nonuniformities, characterized by a high velocity at the centerline and a stagnant zone close to the wall. At higher F_s factors the velocity maldistribution seems to be relatively mild. In nearly all the cases the dimensionless velocity profiles can be approximated as linear with slip at the wall. Correlations are presented to predict the velocity distribution on the tray as a function of the gas rate, and are used together with the retrograde flow model to predict tray efficiency for an industrial size tower.

INTRODUCTION

The increasing use of large-diameter columns in distillation service has brought investigations of the liquid flow patterns on distillation plates, in view of the fact that flow nonuniformities such as stagnant or recirculating zones have been detected experimentally. However, only a few authors have been able to measure these flow nonuniformities. Alesandrov and Vybornov (1971) studied liquid flow on a 1.2 m valve tray air-water simulator. They found clear evidence of a complex flow pattern with dead zones covering between 15 and 26% of the tray area. Later, two independent studies revealed the presence of substantial flow maldistributions on sieve trays. Porter et al. (1972) reported the effect on tray efficiency of stagnant zones observed in a simulator. This work was continued in a series of papers in which the effect of channeling on tray efficiency was studied by means of a theoretical model that includes lateral stagnant zones (Lockett et al., 1973, 1975; Lim et al., 1974). It was concluded from this work that channeling can have a strong effect on tray efficiency of trays of 3 m dia. or greater. At the same time an extensive study of residence time distribution (RTD) on sieve trays in commercial-scale distillation towers in hydrocarbon service was underway at Fractionation Research Incorporated (FRI). The technique and the results were reported by Bell (1972a,b) and demonstrated the presence of remarkably nonideal residence time patterns, and in some cases actual retrograde flow along the sides of the tray.

Bell and Solari (1974) have also proposed a theoretical model that considers a nonuniform velocity distribution in the absence of transverse mixing. The velocity profile is assumed to be an adjustable parameter which depends on the fraction (β) of the tray area carrying the flow in the forward direction (i.e., from inlet downcomer to outlet weir) and the fraction (α) of the net flow to the tray that appeared in the retrograde stream. Neither of these two parameters was known for operating trays. Solari and Bell (1978) extended the retrograde flow model for the case of partial transverse mixing and found that a high degree of transverse mixing was required to overcome the unfavorable effect of velocity gradients on tray efficiency.

Biddulph (1977) and Biddulph and Ashton (1977) have reported eddy diffusivity values from industrial data which indicate that mixing characteristics on each tray vary strongly with the superficial air velocity. Brambilla (1976) also reported from comparison with experimental values that at high values of λEOG, the presence of flow maldistributions emphasizes the effect of vapor mixing, and justifies the actual trend for designing controlled-flow plates to eliminate liquid maldistribution.

At FRI, experiments have been performed that involved controlling the flow by shaping the apron of the inlet downcomer and the outlet weir to prevent retrograde flow. The residence time patterns obtained from the "flow control" tray were nearly ideal, with the isochrons (lines of constant residence time) being almost parallel to each other and to the outlet weir. Similar patterns were obtained by Weiler et al. (1973) on a 7.62 m dia. tray by placing directional slots on the tray.

Yanagi and Scott (1973) have reported the results of the FRI experiments conducted with the flow control sieve trays in a 1.2 m dia. column using a hydrocarbon system. When the results of the experiments using flow control trays were compared to previous experiments with identical sieve trays with standard hardware, under identical operating conditions, it was found that there was very little difference between the overall efficiencies of the two tray designs tested. An explanation for this startling conclusion could be generated by careful selection of the parameters in the theoretical model proposed by Bell and Solari (1974). However, without experimental evidence to relate the parameter values to actual tray performance, such explanation would be at best an arbitrary exercise.

Solari et al. (1982) measured velocity profiles in a 1.25 m air/water simulator using 5% downcomer area sieve trays with 5, 10, and 15% hole area. These experiments showed that the size of the nonuniform flow region ranges from 5 to 60% of the bubbling area, including retrograde flow and stagnant zones.

The study reported in this paper is directed toward measuring the required parameters on commercial-scale trays. To reproduce the column geometry as closely as possible, a 1.22 m dia. air/water simulator was built for this study.

EXPERIMENTAL

Apparatus

The process and instrumentation diagram for the distillation simulator system is shown in Figure 1. The column consists of a bottom receiver 1.22 m in dia. and 1.3 m high, and two column sections 1.83 m long mated to the top of the receiver. In this study there are five trays in the column with the experimental tray being in the center (tray 3). Pressure taps are located so that the pressure drop across individual trays can be measured. Tank-O-Meter's are installed on tray 3 to measure clear liquid height at two positions on the tray. A sight glass is installed to measure the clear liquid height in the downcomer leading to tray 3. The trays are standard commercial sieve trays furnished by FRI, and the design details are summarized in Table 1.

The column is well controlled and conditions can be precisely reproduced. The air flow ranges from shutoff to 1.23 m^3/s at 114.6 kPa absolute pressure. Water can be supplied at flow rates from 3.15×10^{-3} to

Table 1. Tray Details

Tray diameter, m	1.213
Tray spacing, m	0.61
Weir length, m	0.925
Outlet weir height, m	0.05 or 0.10
Downcomer length, m	0.572
Hole diameter and spaces, m	$0.0127 \times 0.05\Delta$
% Bubbling area (over total area)	76
% Hole area (over bubbling area)	5
% Downcomer area (over total area)	12.5

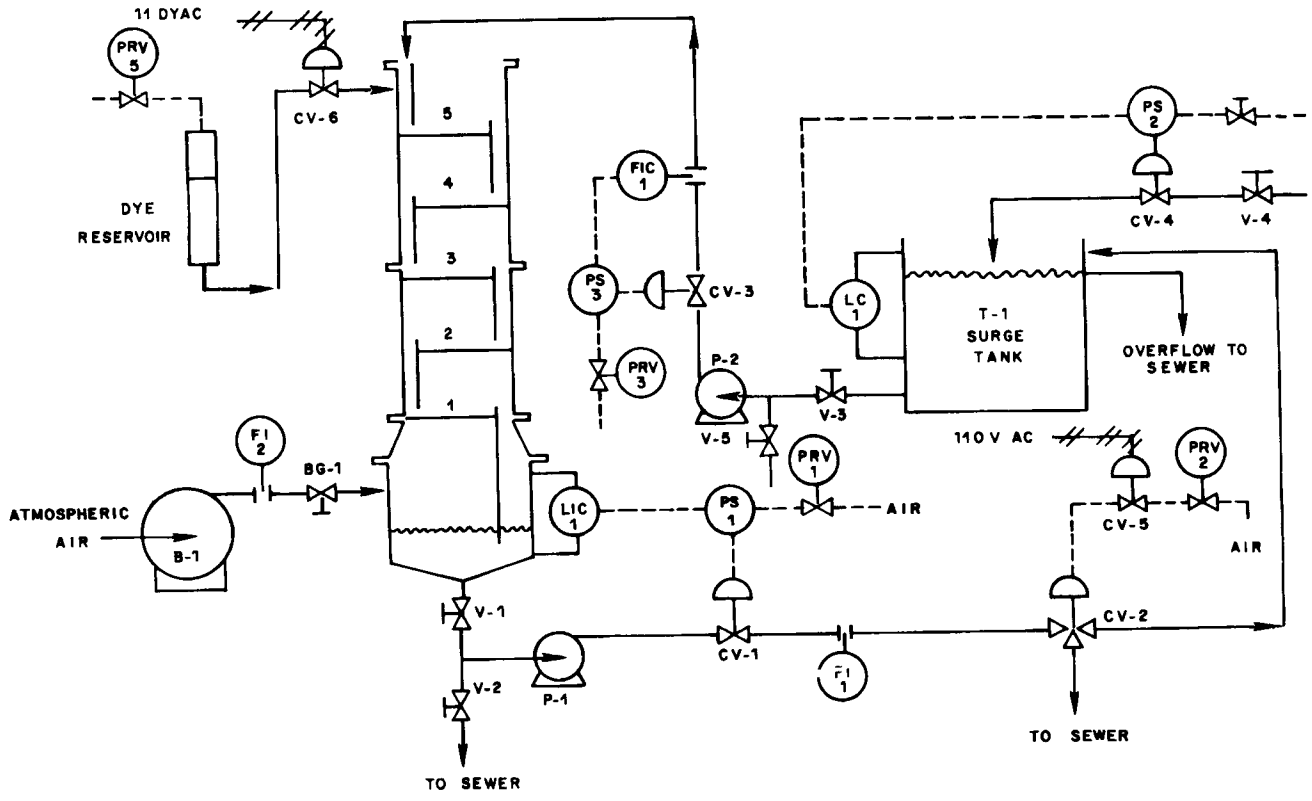

Figure 1. Process and instrumentation diagram of air/water simulator.

18.93×10^{-3} m^3/s. To enable the unit operate at high water-flow rates a 7.4 m^3 surge tank is provided. During startup, the water is recycled to the tank via valve CV-2. During the dye shot experiments the column discharge is sent to the sewer also via valve CV-2, preventing the buildup of a circulating load of dye in the feedwater.

Data Acquisition System

The complete details of the fiber-optic detection system used in this study have been published elsewhere (Bell, 1972a). The data system is based on the use on Uranine dye, which is excited by light coming from one limb of a fiber optic. As the tracer pulse passes the tip of the probe, it is activated and a portion of the fluorescence is transmitted through the second limb of the fiber optic bundle to a photomultiplier tube. From here, the signal is sent to an electrometer/filter amplifier. The amplifier output is serially multiplexed and digitized. The digital signal is converted to a teletype code and transmitted via hard wire to an XDS Sigma 2 computer. The data are logged into storage and at the completion of the run, the zeroeth, first, and second moments and the second central moment (variance) of the concentration time distribution at each probe location are computed. The total time from completion of an experiment to printed results is less than 30 s.

The layout of the 25 light pipes placed in tray 3 and its downcomers is shown in Figure 2. Inside the column, a rectangular frame is installed to hold the probes in place. The tip of the pipe faces the tray surface and is perpendicular to the water flow. It is held about 0.038 m above the floor on the tray and 0.057 m from the floor in the downcomers.

Procedure

Two types of experiments were conducted in this study. The first type was directed to measure residence time distribution (RTD) in the tray and was the same type as those reported by Bell (1972b). The dye pulse was injected into the downcomer leading to tray 4. The injection time was 1 s for all the experiments. The pulse response was simultaneously detected in 22 channels (probes 1 to 22) corresponding to the probe layout given in Figure 2. Data were read at a rate of 0.04545 s per channel, which means that each channel was sampled each 1 s. In this way the concentration-time curve at each probe is stored in the computer as a series of points separated by discrete time intervals.

A special set of experiments was designed to measure the RTD in the downcomers. In these experiments only the five probes located in the downcomers (probes 19, 20, 21, 22, and 23) were monitored.

The second kind of experiment was designed specifically to measure the linear velocity across the tray by injecting a pulse of dye on tray 3 just outside the downcomer apron and in line with a longitudinal row of probes. A pulse of dye was injected at one of the four injection points located at the same position as probes 1, 2, 3, and 4 (see Figure 2). The injection time was 0.2 s. Only the pulse responses from the four probes in line with the injection points were monitored at a sample rate of 0.2 s per channel.

From the moments of the resultant RTD's the average velocity of the fluid was calculated by dividing the distance between two consecutive probes located in the same longitudinal row by the difference in mean residence time between the two probes. Referring to Figure 2, velocities were determined between the probe line composed of probes 5, 6, 7, 8 and probe line 9, 10, 11, 12, respectively. Velocities were also measured between this last probe line and the line 13, 14, 15, 16, respectively. The first calculation yields an average velocity distribution in the middle section of the tray, the second approximates the velocity distribution at the tray outlet.

RESULTS AND DISCUSSION

Experimental results obtained from measuring tray clear liquid heights at different gas and liquid flow rates were correlated by regression analysis to fit the following prediction equation.

$$b = 1.4 \times 10^{-2} + 0.4h_w + 2.21L_w - 0.0135F_s \qquad (1)$$

The coefficient for the outlet weir height h_w was obtained by comparing the data for 0.05 and 0.1 m weir heights. This factor is double the value given in the AIChE (1958) correlation to

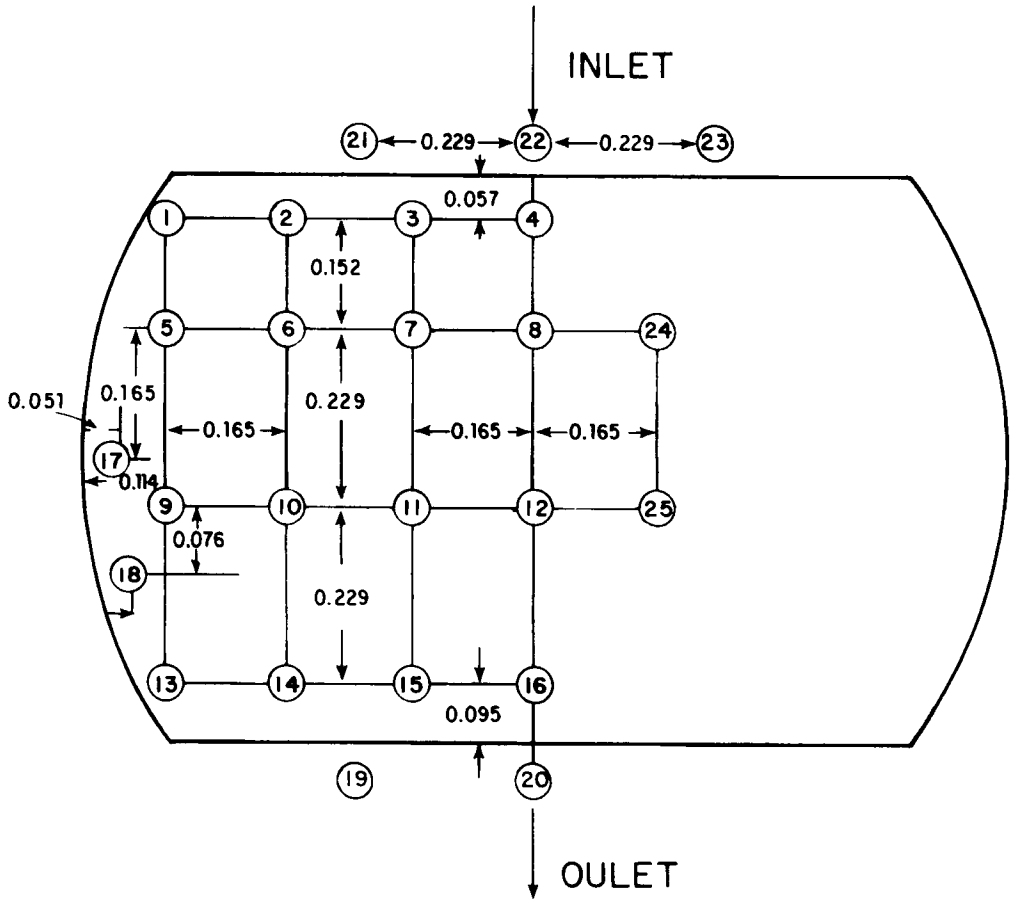

ALL DISTANCES IN METERS

Figure 2. Probe layout for tracer detection on tray number 3.

predict liquid holdup. Flow dependence of the clear liquid level was found to be very similar to the prediction of the AIChE, which gives coefficients 2.45 for L_w and -0.0135 for F_s.

Data Reproducibility

In order to check data reproducibility, a series of 16 replicates for a typical RTD experiment was performed under exactly the same flow conditions. The average of the four average replicates together with the standard deviation and the percent of standard deviation were calculated for 20 channels. The average deviation between replicates was 2.9% for the mean residence time and 15.8% for the second central moments. For the purpose of this study, these percent deviations indicate a sufficient degree of data reproducibility. Sampling rate was found not to have an important effect in data accuracy. In fact, the results did not show a continuous decay as the sample rate was increased, but rather they reflected the random behavior of the system.

Data reproducibility of the velocity determination experiments was also studied. Two sets of experiments at two different flow conditions were replicated four times each, and reproducibility was analyzed both for the mean residence time and velocity results. The two flows were selected to represent conditions of low and high dispersion on the liquid phase.

The standard deviation for the FNM values ranged from 0.9 to 11.5%, at an average of 5.4%. This gives a good estimation of the reproducibility of the mean residence time used to evaluate the velocity between consecutive probes. As a conclusion of this reproducibility analysis it can be said that the average error in the velocity determination is less than 10%.

Residence Time Distribution Results

Typical results from the RTD experiments are presented in Figure 3 as a set of plots mapping the residence time and variance distributions on the tray for different flow conditions. Residence time profiles were obtained by tracing lines of constant residence time (isochrons) across the 18 probes located on the tray. Lines of constant variance were obtained in a similar fashion to map mixing patterns on the tray.

The distinctive feature of these profiles is the zone of extended residence time and variance near the wall and the relatively shorter residence time and variance near the centerline. This is particularly evident at low liquid and gas load where an actual pooling of liquid seems to occur. The pooling conditions, characterized by lines of high residence time and variance at the wall, are more severe at low gas flow rates. The effect of an increasing water flow rate in this case is limited to reduce the pooling zone to a narrower extension. As the gas rate increases, the pooling region is shifted toward the outlet weir until it almost vanishes at the highest gas load. These results suggest that mixing patterns on the tray are far from uniform, and zones of different degrees of mixing are present on the tray.

The residence time and variance profiles obtained in this

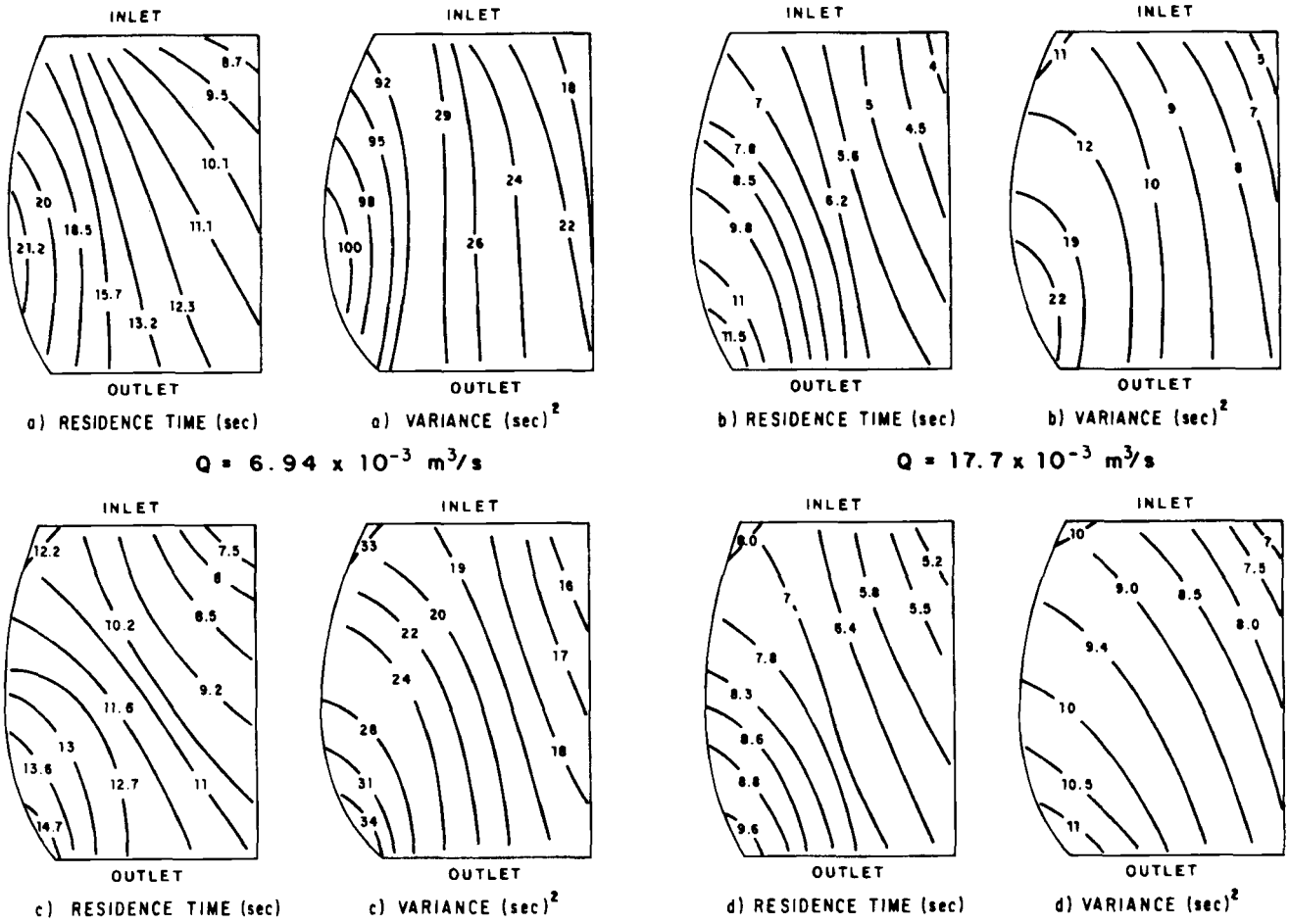

Figure 3. RTD and variance profiles: a) $F_s = 0.462$; b) $F_s = 0.655$; c) $F_s = 1.105$; d) $F_s = 1.464$.

study are almost identical to the patterns observed in the FRI experiments reported by Bell (1972b). The FRI results indicate the existence of pooling zones at F_s greater than those for which pooling ceased to exist in our study for equivalent liquid flow rates. For example, Bell found extensive zones of high residence times at $F_s = 0.699$ for a liquid load of 7.06×10^{-3} m³/s. In our experiments, at the same flow conditions, the pooling zones were smaller and shifted toward the outlet weir. This difference probably arises from the difference in tray designs used in the respective experiments.

Effect of Liquid and Gas Flow Rate

Figures 4 and 5 illustrate the variation of mean residence time and variance, respectively, along the transverse direction of the tray for different F_s factors. These values are for the probes located over the transverse centerline of the tray. Both figures show sharp gradients in the transverse direction at low F_s factors. As F_s increases the crossplot curves become more flat, showing an appreciable reduction in the transverse gradient. Note that mean residence times tend to increase at the centerline and decrease near the wall as the gas rate increases.

The dimensional variance σ^2 at a given position on the tray is affected both by convective and turbulent dispersion effects. There is little doubt that the high variance at low air flow rates is caused by the presence of pooling regions near the wall. The effect of an increase in vapor load appears to be to destroy these pools, thereby producing a more uniform lateral mixing. In general, for those flow conditions in which convection is the

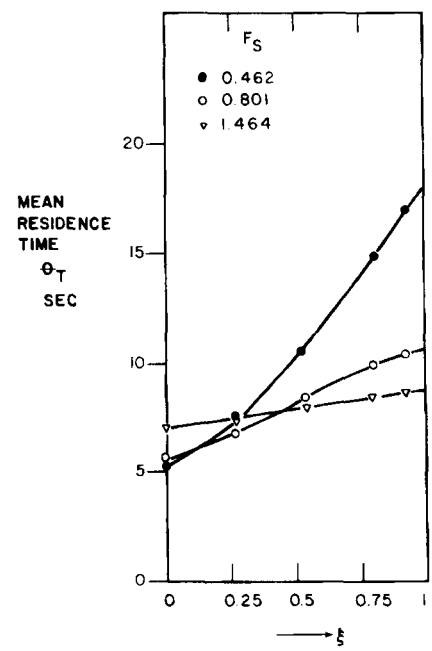

Figure 4. Mean RTD along transverse centerline of tray, $Q = 13.9 \times 10^{-3}$ m³/s.

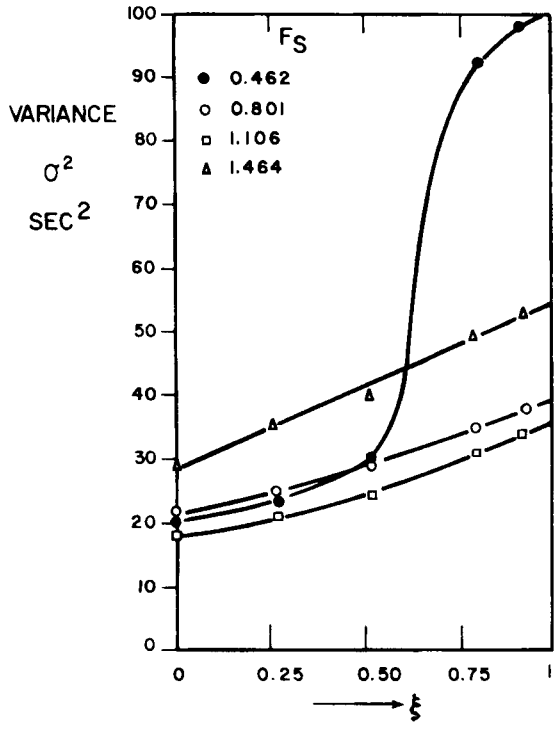

Figure 5. Lateral variance profile along transverse centerline of tray, $Q = 6.94 \times 10^{-3}$ m³/s.

predominant effect, the variance shows a continuous decrease with an increasing gas rate, as can be observed in Figure 5. However, as the flow conditions become such that the turbulence created by the violent action of the vapor overcomes the convective effect, any further increase in gas load will produce more turbulence, therefore increasing the amount of turbulent mixing. This explains the minimum observed in Figure 5 as F_s increases.

The results reported here are in apparent contrast with most of the previous studies. The reason that previous researchers only observed an increase in mixing with increasing F_s factor is that in most cases small rectangular simulators were used, in which pooling zones and nonuniform velocity distribution are not likely to develop. Barker and Self (1962) have reported that a W-shaped curve is noticed in a plot of the mixing parameter E against the F_s factor at low values. The explanations found in the literature accredited this unusual behavior to gas velocity effects on froth structure.

Figure 6 is a plot of the difference between the mean residence times at the centerline and at the column wall as a function of F_s factor at different water flow rates. Although there is a significant scattering in the data, the decay in the lateral gradient as F_s increases can approximately be described by the same curve for all the water flow rates. Perhaps these gradients are somewhat lower at the highest water flow rates, but the relationship is not clear and the data suggest a random behavior.

The residence time profiles obtained in these experiments contain the effect of the tray above and downcomers. In an attempt to isolate the overall mean residence time for the test tray, the differences between the FNM's from the two downcomers were calculated. In Figure 7 the overall tray mean residence time $\Delta\theta_o$ is presented as a function of the air and water flow rates. The overall difference $\Delta\theta_o$ was calculated as the average of $\Delta\theta_{DS}$ and $\Delta\theta_{DC}$, which represent the differences of the FNM's between probes 19 and 21 at the sideline, and probes 20 and 22 at the centerline, respectively. Figure 7 shows that $\Delta\theta_o$ decreases sharply with the liquid load, as could be expected since the mean residence time is related inversely to the liquid flow rate and directly to the tray clear liquid height. The F_s factor seems to have little effect on the overall tray mean residence time despite the fact that an increase in gas rate causes a decrease in tray clear liquid level.

It is clear from these graphs that the gas rate has a strong influence on the liquid flow patterns in the tray. Although the residence time is directly proportional to the water rate, the liquid load has less influence in shaping the flow distribution than does the gas flow rate.

Velocity Distribution

Typical velocity distribution curves obtained from the velocity determination experiments are presented in Figure 8. The dimensionless velocity distribution shown in Figure 9 was calculated by dividing the linear velocity by the volumetric average velocity. The underlying profiles show that the linear velocity at the centerline is between 1.1 to 2.8 times the average velocity, depending on the flow conditions. The velocity at the wall is only a fraction of the average velocity.

Although the pattern of isochrons seemed indicative of more

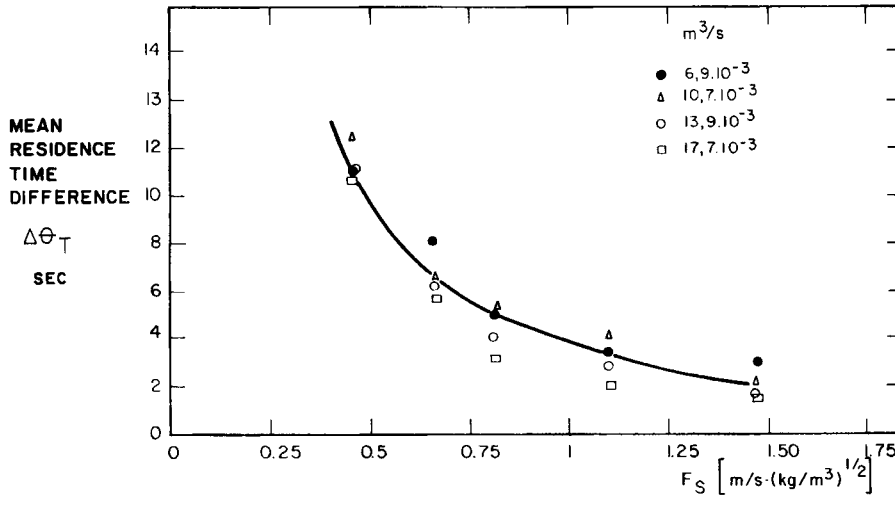

Figure 6. Difference between mean residence time at centerline and at wall as a function of F_s factor.

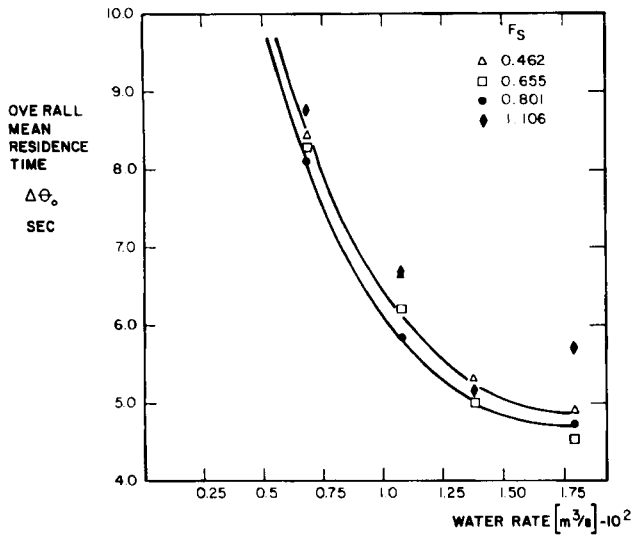

Figure 7. Overall residence time as a function of water flow rate.

severe flow nonuniformities, the underlying velocity maldistribution seems to be relatively mild except at low gas rates. The velocity profiles at low F_s factors show severe flow nonuniformities characterized by a high velocity at the centerline and a stagnant zone close to the wall. The variance in this region was as large as 60 s^2 which is almost 25 to 30 times the variance in the forward-flow region. Evidently, in this condition of high dispersion any attempt to evaluate the linear velocity lacks significance. Therefore, the velocities were assumed to be zero in the zones of high dispersion, as shown in Figure 9. However, the presence of zones of high residence time and variance does not necessarily mean that the zones are stagnant. There is also the possibility of liquid recirculation, which could cause the same type of profile. To clear up this point, dye was injected at probe positions 13, 18, and 17, showing only a very weak response in the probes back to the injection points. These results show no evidence of recirculation flow, but rather indicate the presence of stagnant zones with some degree of backmixing due to the random movement of liquid particles caused by the bubbling action of the gas. However, the same experiments performed with a blanked tray, in the absence of air flow, gave strong evidence of flow recirculation. In the water table experiments, most of the dye injected at position 18 was detected back in positions 17, 5, and 1. Dye injection at positions 3 and 4 also showed strong signals at positions 17 and 18, which has not been observed in the air/water froth experiments.

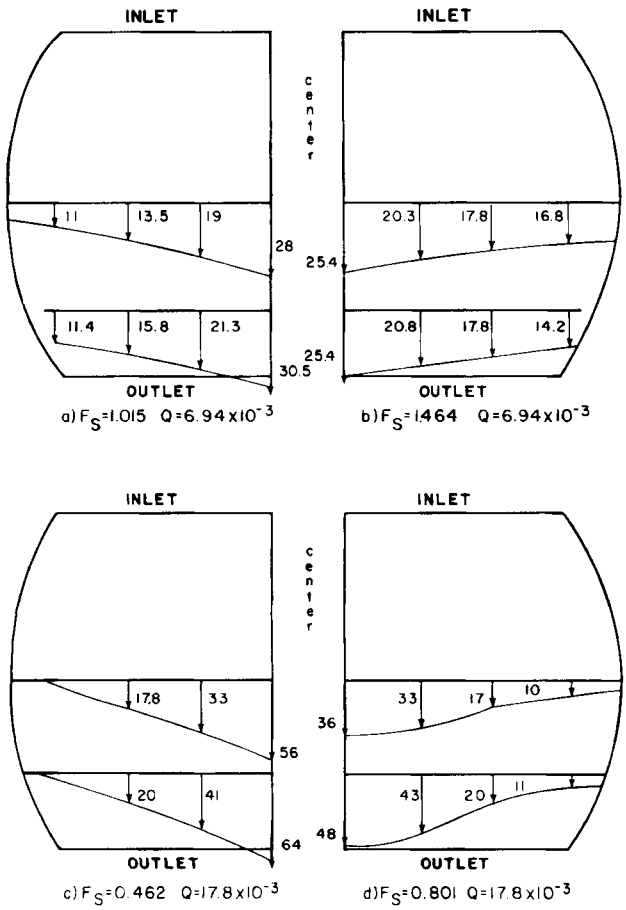

Figure 8. Velocity distribution, m/s.

As both the gas and liquid rates are increased, flow nonuniformities are reduced but not completely eliminated. At the highest gas rates, even though there continues to be smaller velocities at the wall, the velocity distribution curves become more nearly flat and the pooling tendency is almost completely eliminated. This behavior could be explained by considering that the net effect of an increase of gas flow rate would be to displace part of the high volumetric flow in the centerline toward the column wall, thereby improving the flow distribution on the tray.

The effect of an increase in liquid flow rate is to increase the dimensional velocity. However, the liquid velocity is not directly proportional to the liquid rate, due to the increase in tray clear liquid level with water rate. It is clear then, that the effect of the gas is fundamental in the underlying flow patterns that describe the route by which the liquid travels from inlet to outlet. This is determined by the momentum of the gas jets flowing through the tray holes. The momentum or energy introduced by the gas tends to brake the recirculation pattern and to displace the liquid near the wall at a higher velocity.

Since an increase in hole area and a reduction in weir length will decrease the gas velocity for the same gas flow rate, it should be expected that for tray geometries with higher percentages of hole area and shorter weir lengths, retrograde flow will likely be much more severe. Probably this was the case for the experiments reported by Bell (1972b) in a FRI tray with an 8% hole area, where flow recirculation was evident.

The dimensionless velocity profiles obtained in these experiments can be approximated as linear with slip at the wall in nearly all the cases. It was also verified that they are independent of the liquid flow rate since any difference is within experimental error (± 10%). Therefore, by assuming a linear distribution and considering the dimensionless velocity profiles as a function only of the gas rate, a one-parameter correlation can be approximated to describe the velocity distributions.

In Figure 10, the dimensionless velocity at the tray center $q(0)$ has been plotted against the F_s factor. The relationship between these two parameters can be expressed by the following equation:

$$q(0) = 1.53(F_s)^{-0.59} \tag{2}$$

The fractional slip velocity q_s, defined by the ratio of wall velocity to mean velocity, is given by the following equation for the cases in which the entire tray is carrying the forward flow,

$$q_s = 2 - q(0) \tag{3}$$

The velocity maldistribution can then be estimated for a given set of flow conditions by replacing q_s in Eq. 4.

$$q(\xi) = 2(1 - q_s)(1 - \xi) + q_s \tag{4}$$

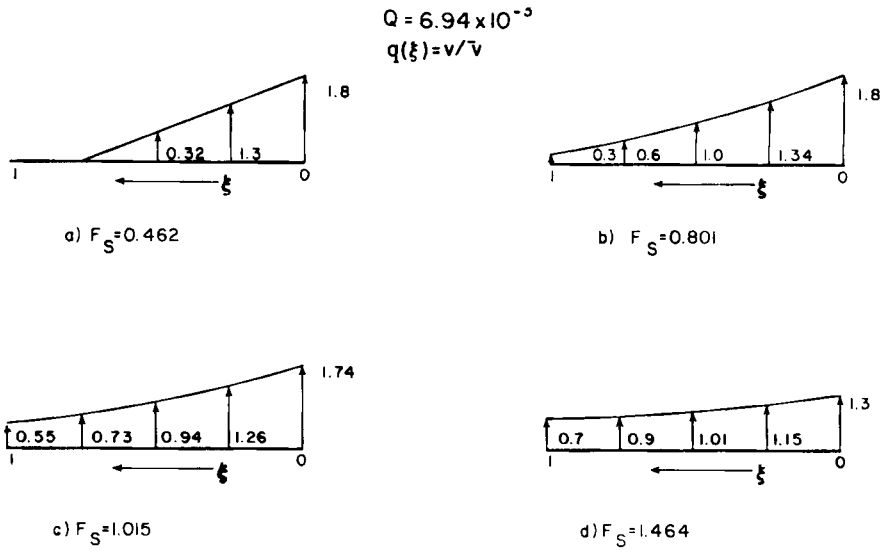

Figure 9. Dimensionless velocity profiles as a function of gas flow rate.

Figure 10 shows that at F_s factors lower than 0.65 the central velocity $q(0)$ is larger than 2. According to Eq. 3, the slip velocity should be negative, which would indicate the presence of retrograde flow. Since no evidence of significant retrograde flow was found with the tray being studied, this result suggests that the velocity profiles at F_s factors lower than 0.65 may be represented by a forward flow region with a linear velocity profile flanked by stagnant zones with zero velocity, according to Eq. 5:

$$q(\xi) = \frac{2}{\beta^2}(\beta - \xi)\xi \leq \beta \tag{5}$$

where β represents the area fraction of forward flow and can be calculated as:

$$\beta = \frac{2}{q(0)} \tag{6}$$

Since $q(0)$ is independent of liquid rate, the area fraction of forward flow, β, will depend only on the gas rate. It should be kept in mind that the velocity profile is also a function of the tray geometry, therefore the correlations presented here are limited only to sieve trays with 5% hole area and 12.5% downcomer area.

Efficiency Prediction

The experimental evidence gathered in this study enables us to use the theoretical model presented in our previous papers (Bell and Solari, 1974; Solari and Bell, 1978) to analyze efficiency data from industrial operation of fractionating units. For those cases in which the entire tray is carrying the forward flow the value of β is unity and the fractional retrograde flow, α, is zero. Given these values it is now possible to determine the theoretical effect on efficiency.

Experiments performed by Yanagi and Scott (1973) at FRI showed very small differences in tray efficiency for trays with uniform and nonuniform flow. The Peclet numbers reported in the FRI experiments using organic systems, as well as that calculated here for the air/water experiments, were in excess of 30

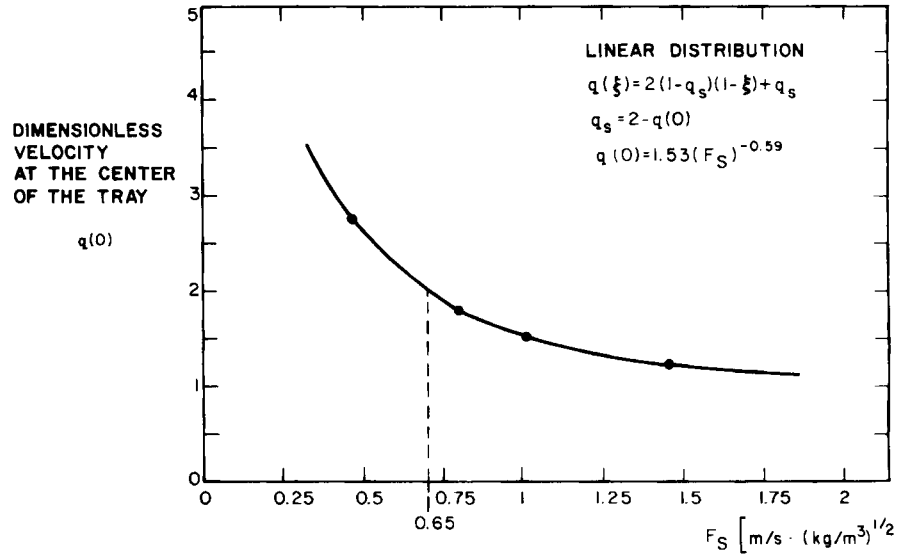

Figure 10. Dimensionless velocity at tray center as a function of gas flow rate.

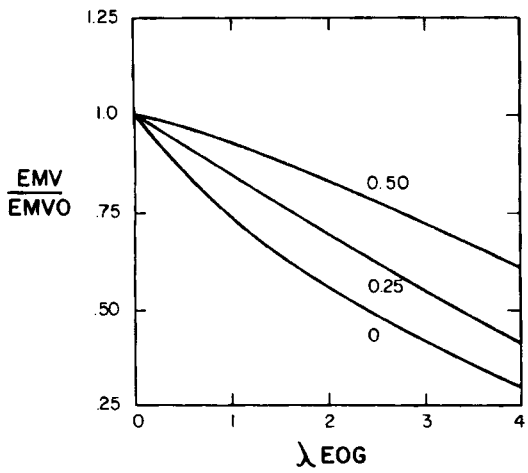

Figure 11. Murphree tray efficiency as a function of λEOG.

and therefore could be taken as infinite. The values of λEOG for the FRI studies were in the range of 0.7 and the F_s factor was around 0.975. Figure 11 is a plot of the ratio of Murphree tray efficiency, *EMV*, (Bell and Solari, 1974) for a tray on which a linear velocity distribution exists, to the ideal efficiency, *EMVO*, obtained assuming uniform velocity distribution. The parameter is the fractional slip velocity at the wall for the linear distribution at Peclet number infinite. For $F_s = 0.975$, Eqs. 2 and 3 yield a q_s of 0.38, and for $\lambda EOG = 0.7$ the *EMV/EMVO* ratio from Figure 11 is about 0.95. The predicted increase in efficiency by exactly correcting a tray to uniform flow conditions is therefore 5%. Considering the fact that the flow control tray retained some flow nonideality, and considering experimental error, it now appears that large changes in efficiency should not have been expected.

In order to use these results in tray design practice, more experimental work is still required, especially to obtain correlations to predict tray velocity distribution as a function of tray geometry, system properties, and operating conditions. Solari et al. (1982) have already initiated experimental work oriented in this direction that has shown the feasibility of obtaining such correlations.

ACKNOWLEDGMENT

The authors acknowledge partial support of FONINVES through Grant A-37 and National Science Foundation through MSFGK 30370.

NOTATION

b = clear liquid height in tray, m
D = tray diameter, m
E = turbulent eddy diffusivity
EMV = overall Murphree tray efficiency
$EMVO$ = ideal Murphree tray efficiency
EOG = Murphree point efficiency
$F_s = V \cdot \rho_v^{1/2}$, m/s(kg/m^3)$^{1/2}$
FNM = first normalized moment, s
h_w = outlet weir height, m
L_w = volumetric liquid flowrate/average tray width, m^2/s
P_e = Peclet number
Pe_z = Peclet number in the flow direction
$P_{e\xi}$ = Peclet number in the transverse direction
$q(\xi)$ = normalized velocity distribution function
$q(0)$ = normalized velocity at the tray center
q_s = slip velocity at the wall
Q = liquid volumetric flowrate, m^3/s
V = superficial vapor velocity, m/s
U = linear liquid velocity, cm/s
$\overline{U}$ = average liquid velocity, cm/s
Z = dimensionless ordinate in the liquid flow direction

Greek Letters

α = volumetric fraction of liquid recycled
β = forward flow area/active area of the tray
λ = ratio of the slope of the equilibrium line to the operating line
ξ = dimensionless ordinate in the direction normal to flow
Δ = difference operator
ρ_v = vapor density
σ^2 = dimensional variance, s^2
SCM = second central moment
θT = mean residence time, s
$\Delta\theta_o$ = overall mean residence time, s
$\Delta\theta_T$ = mean residence time difference, s

LITERATURE CITED

AIChE, *Bubble Tray Design Manual: Prediction of Fractionation Efficiency*, AIChE, New York (1958).
Aleksandrov, I. A., and V. G. Vybornov, "Investigation of the Hydrodynamic Pattern of Liquid Flow on Crossflow Trays," *Teor. Osnovy Kim. Tekh.*, **5**, 339 (1971).
Barker, P. E., and M. F. Self, "The Evaluation of Liquid Mixing Effects on a Sieve Plate Using Unsteady and Steady State Tracer Techniques," *Chem. Eng. Sci.*, **17**, 541 (1962).
Bell, R. L., "Experimental Determination of Residence Time Distributions on Commercial-Scale Distillation Trays Using a Fiber Optic Technique," *AIChE J.*, **18**, 491 (1972a).
——, "Residence Time and Fluid Mixing on Commercial-Scale Sieve Trays," *ibid*, **18**, 498 (1972b).
Bell, R. L., and R. B. Solari, "Effect of Nonuniform Velocity Fields and Retrograde Flow on Distillation Tray Efficiency," *ibid*, **20**, 688 (1974).
Biddulph, M. W., "Tray Efficiency is Not Constant," *Hydrocarbon Processing*, **145**, (Oct., 1977).
Biddulph, M. W., and N. Ashton, "Deducing Multicomponent Distillation Efficiencies from Industrial Data," *Chem. Eng. J.*, **14**(1), 7 (1977).
Bolles, W. L., "Estimating Valve Tray Performance," *Chem. Eng. Progr.*, **72**(9), 43 (1976).
Brambilla, A., "The Effect of Vapor Mixing on Efficiency of Large-Diameter Distillation Plates," *Chem. Eng. Sci.*, **31**, 571 (1976).
Fell, C. J. D., and W. V. Pinczewski, "New Considerations in the Design and Operation of High-Capacity Sieve Trays," *Chem. Eng.*, **316**, 45 (1977).
Garrett, G. R., R. H. Anderson, and M. Van Winkle, "Calculation of Sieve and Valve Tray Efficiency in Column Scale-up," *Ind. Eng. Chem. Proc. Des. Dev.*, **16**(1), 79 (1977).
Lim, C. T., K. E. Porter, and M. J. Lockett, "The Effect of Liquid Channeling on Two-Pass Distillation Plate Efficiency," *Trans. Inst. Chem. Engrs.*, **52**, 193, (1974).
Lockett, M. J., C. T. Lim, and K. E. Porter, "The Effect of Liquid Channeling on Distillation Column Efficiency in the Absence of Vapor Mixing," *Trans. Inst. Chem. Engrs.*, **51**, 281 (1973).
Lockett, M. J., K. E. Porter, and K. S. Bassoon, "The Effect of Vapor Mixing on Distillation Plate Efficiency when Liquid Channeling Occurs," *Trans. Inst. Chem. Engrs.*, **53**, 125 (1975).
Porter, K. E., M. J. Lockett, and C. T. Lim, "The Effect of Liquid Channeling on Distillation Plate Efficiency," *Trans. Inst. Chem. Engrs.*, **50**, 91 (1972).
Sohlo, J., and S. Kinnunen, "Dispersion and Flow Phenomena on a Sieve Plate," *Trans. Inst. Chem. Eng.*, **55**, 71 (1977).
Solari, R. B., and R. L. Bell, "The Effect of Transverse Eddy Dispersion

on Distillation Efficiency," AIChE 84th Natl. Meet., Atlanta, Paper 46f (1978).
Solari, R. B., et al., "Velocity Distribution and Liquid Flow Patterns on Industrial Sieve Trays," *Chem. Eng. Commun.*, 13, 369 (1982).
Weiler, D. W., W. V. Delnicki, and B. L. England, "Flow Hydraulics of Large-Diameter Trays," *Chem. Eng. Prog.*, 69, 67 (1973).
Yanagi, T., and B. D. Scott, "Effect of Liquid Mixing on Sieve Trays," *Chem. Eng. Prog.*, 69, 75 (1973).

Manuscript received June 29, 1982, and revision received Apr. 18, 1985.